Characteristics of photonic bands generated by quadrangular multiconnected networks*

Luo Rui-Fang(罗瑞芳)[a], Yang Xiang-Bo(杨湘波)[a)b)†], Lu Jian(卢 剑)[a], and Liu Timon Cheng-Yi(刘承宜)[b]

[a] *Key Laboratory of Laser Life Science and Institute of Laser Life Science of Ministry of Education, College of Biophotonics, South China Normal University, Guangzhou* 510631, *China*

[b] *School of Physical Education and Sports Science, South China Normal University, Guangzhou* 510006, *China*

(Received 13 March 2013; revised manuscript received 2 April 2013)

In this paper, by means of the network equation and generalized dimensionless Floquet–Bloch theorem, we study the influences of the number of connected waveguide segments (NCWS) between adjacent nodes and the matching ratio of waveguide length (MRWL) on the photonic bands generated by quadrangular multiconnected networks (QMNs), and obtain a series of formulae. It is found that multicombining networks (MCNs) and repetitive combining networks (RCNs) are equivalent to each other and they can all be simplified into the simplest fundamental combining systems. It would be useful for adjusting the number, widths, and positions of photonic bands, and would possess potential applications for the designing of all-optical devices and photonic network devices.

Keywords: photonic band gap, waveguide network, multiconnected network

PACS: 42.70.Qs, 42.79.Gn, 41.20.Jb **DOI:** 10.1088/1674-1056/22/10/104211

1. Introduction

The dielectric structures with spatial periodicities are capable of exhibiting a photonic band gap (PBG), where the propagation of electromagnetic (EM) waves with certain frequencies is inhibited.[1,2] PBG materials have had extensive applications in the new optical devices, and so, they have attracted much attention.[3–6] PBG materials open up new research fields for condensed matter physics, optics, material science, etc. The fundamental investigations include PBG structures,[4,7–10] properties of transmission and reflection,[11–13] photonic waveguides,[14–16] phenomena of negative refraction,[17–19] defect states,[20–22] photonic tunneling effect,[23,24] etc.

As the lattice constant of a PBG is on the scale of the wavelengths of EM waves, the shorter the working wavelength, the smaller the characteristic length of PBG is and then the more difficult to fabricate the structures will be, especially for three-dimensional (3D) structures. However, for those PBG networks composed of one-dimensional (1D) waveguides,[25,26] their structures are flexible and the number and length of the waveguides[25–28] between adjacent nodes can be adjusted. Furthermore, the phase, amplitude, and wave function at each node can be easily accessible. In addition, strong scattering can be easily introduced into a unit cell to produce large full stopbands in any dimension.[25] Based on the aforementioned advantages, it is very convenient for the PBG networks to accomplish experimental investigations. Therefore, researchers have paid much attention to the structures of this kind. So far, many properties of quasi-1D,[26,29] two-dimensional (2D),[27,30] and 3D[25,27] PBG networks have been studied, which include defect state mode,[31] random scattering,[32] slow light effect,[33] band gap structure,[26,27,34] nonlinear optical effect,[35] etc.

To the best of our knowledge, for those PBG networks composed of 1D waveguides, adding more segments between adjacent nodes is equal to introducing more loops,[25,28] and consequently, the possibility of producing resonance and antiresonance would be increased. Recently, we studied quadrangular multiconnected networks (QMNs) and found that the largest attenuation may appear near the edge of the narrow passbands rather than in the center of the stopbands.[28] Moreover, we further studied the photonic band properties of two-segment-connected networks (2SCNs) and three-segment-connected networks (3SCNs).[36] However, the band structures of the more complex networks, where all the adjacent nodes are connected by more than three segments, have not been studied in detail. And the investigation of equivalence property among the multiconnected combining networks (CNs) have not been reported yet. Then what are the band structures of the complex multiconnected networks (MNs)? And what are the concrete rules of the number, widths, and positions of the photonic bands? These are interesting problems and the answers would possess potential applications in designing all-optical devices and photonic network devices.

As one of the work series of our group, in this paper we investigate the photonic band characteristics of multicombining networks (MCNs) and repetitive combining networks (RCNs). It is found that their photonic bands are equivalent to those of the fundamental combining networks (FCNs). Us-

*Project supported by the National Natural Science Foundation of China (Grant No. 10974061).

†Corresponding author. E-mail: xbyang@scnu.edu.cn

© 2013 Chinese Physical Society and IOP Publishing Ltd

ing this property, people can greatly simplify the networks of this kind or the systems which contain the subnetworks of this kind. Furthermore, we also obtain a series of formulae for the band number, widths, and positions. With these formulae people can design a waveguide network to generate a specified number of photonic bands at the specified frequency positions. It would be useful in designing all-optical devices and photonic network devices.

The rest of this paper is organized as follows. In Section 2, we mainly introduce the model of the QMN and the theory for studying the mentioned networks. In Section 3, we present the numerical results and discuss the number, widths, and positions of photonic bands generated from the QMNs. Finally, some conclusions are drawn from the present study in Section 4.

2. Model and theory

The QMN studied is shown in Fig. 1, where each dashed line connecting adjacent nodes denotes n types of waveguide segments with the lengths of $d_1, d_2, \ldots, d_n$, respectively. So only the monomode propagation of EM waves needs to be considered. The EM wave function in any segment between nodes i and j can be regarded as a linear combination of two opposite traveling plane waves: $\psi_{ij} = \alpha_{ij}\mathrm{e}^{\mathrm{i}kx} + \beta_{ij}\mathrm{e}^{-\mathrm{i}kx}$, where $k = \omega/c$ is the wave vector, ω is the angular frequency and c is the speed of EM waves in the vacuum. Furthermore, at any node i, the energy flux conservation law gives

$$\sum_{j=1}^{n} \psi_{ij} \frac{\partial \psi_{ij}}{\partial x} A_{ij}\big|_{x=0} \frac{1}{\mu\omega} = 0. \tag{1}$$

Then, one can obtain the following network equation:[37]

$$-\psi_i \sum_{j=1}^{n} \cot(kl_{ij}) + \sum_{j=1}^{n} \psi_j \csc(kl_{ij}) = 0, \tag{2}$$

where cot and csc are the cotangent and cosecant functions, respectively, $\psi_i(\psi_j)$ is the wave function at node $i(j)$, l_{ij} is the length of the waveguide between nodes i and j, and the summation of j is taken over all of the nodes linked directly to node i.

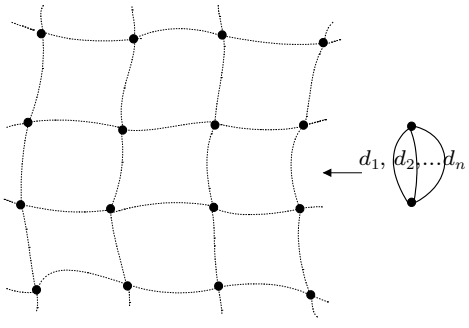


Fig. 1. The QMN, where each dashed line connecting adjacent nodes denotes n types of waveguide segments with the lengths of $d_1, d_2, \ldots, d_n$, respectively.

The QMN investigated in this paper does not possess spatial translation periodicity and only has configuration translation periodicity, and consequently, we study its photonic band properties by means of the generalized dimensionless Floquet–Bloch theorem we proposed recently, which is shown as follows:[28]

$$\psi_{\boldsymbol{K}}(\boldsymbol{N}+\boldsymbol{T}) = \psi_{\boldsymbol{K}}(\boldsymbol{N})\mathrm{e}^{\mathrm{i}\boldsymbol{K}\cdot\boldsymbol{T}}, \tag{3}$$

where $\boldsymbol{N}$ is the node index vector, $\boldsymbol{T}$ is the configuration translation vector, $\boldsymbol{K}$ is the configuration 'wavevector', and they are all dimensionless.

By means of Eqs. (2) and (3), the dispersion relation of the network in Fig. 1 can be obtained as

$$\cos K_1 + \cos K_2 = f(k), \tag{4}$$

where

$$f(k) = \frac{2\sum\limits_{j=1}^{n} \cot(kd_j)}{\sum\limits_{j=1}^{n} \csc(kd_j)}, \tag{5}$$

and K_1 and K_2 are the two components of the configuration 'wavevector' $\boldsymbol{K}$.

3. Numerical results and discussion

In this section, we give the numerical results for the properties of photonic bands generated from certain QMNs with integer matching ratios and non-integer matching ratios of waveguide length (MRWLs).

3.1. Networks with integer MRWLs

The rules for the number, widths, and positions of photonic bands generated from the 3SCNs with arbitrary MRWLs are complex, therefore, general rules cannot be obtained. As a result, in Subsection 3.1.1 only the properties of photonic bands for the 3SCNs with $d_3{:}d_2{:}d_1 = n^i{:}n^j{:}1$ are presented.

Similarly, the properties of the photonic bands generated by the MNs with arbitrary MRWLs where the number of connected waveguide segments (NCWS) between adjacent nodes is bigger than three are also complex, and consequently, it is difficult to obtain the general rules. However, there exist the MNs of this kind, which are closely related to each other, and those are what we call CNs in Subsection 3.1.2. The properties of their photonic bands are relatively simple, and in Subsection 3.1.2 we give out the analytical rules.

3.1.1. 3SCNs with $d_3{:}d_2{:}d_1 = n^i{:}n^j{:}1$

It is found that when i is a positive integer and j is a natural number smaller than or equal to i, the 3SCNs with $d_3{:}d_2{:}d_1 = n^i{:}n^j{:}1$ only generate wide bands.

(i) When n is even, the numbers of wide passbands and wide stopbands are, respectively,

$$m_{\mathrm{wp}} = 2n^i \tag{6}$$

and

$$m_{\rm ws} = 2n^i - 1. \tag{7}$$

(ii) When n is odd, the numbers of wide passbands and wide stopbands are

$$m_{\rm wp} = 2n^i - 1 \tag{8}$$

and

$$m_{\rm ws} = 2n^i - 2, \tag{9}$$

respectively.

As examples, we calculate the two networks with $n = 2$, $i = 3$, $j = 2$ and $n = 3$, $i = 2$, $j = 1$, respectively. The results are shown in Fig. 2, where the symmetry points Γ, X, and M correspond to the wave vectors $(K_1, K_2) = (0,0)$, $(\pi,0)$, and (π,π), respectively. In Fig. 2(a), d_3:d_2:$d_1 = 2^3$:2^2:1, there exist 16 passbands and 15 stopbands. In Fig. 2(b), d_3:d_2:$d_1 = 3^2$:3:1, 17 passbands and 16 stopbands are created. The numerical results accord with Eqs. (6)–(9).

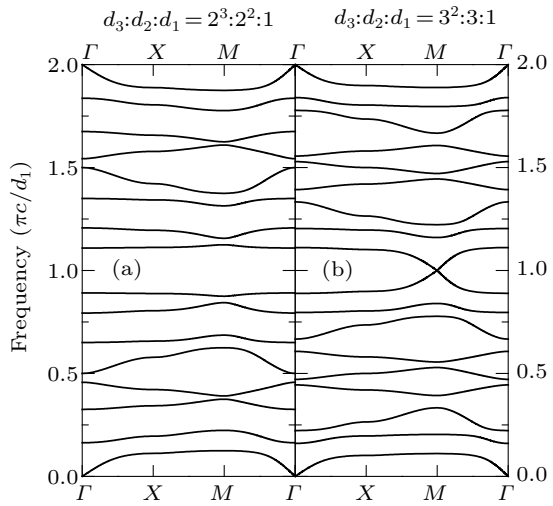


Fig. 2. Band structures of 3SCNs. (a) d_3:d_2:$d_1 = 2^3$:2^2:1 and 16 wide passbands and 15 wide stopbands are created. (b) d_3:d_2:$d_1 = 3^2$:3:1 and 17 wide passbands and 16 wide stopbands are produced.

3.1.2. CNs

For convenience, we simplify $\overbrace{n:n:\ldots:n}^{m}$ as $n^{(m)}$ and define the networks with $d_{m(i_1+i_2+\ldots+i_k)} : d_{m(i_1+i_2+\ldots+i_k)-1} : \cdots : d_2 : d_1 = n_1^{(i_1 m)} : n_2^{(i_2 m)} : \cdots : n_{k-1}^{(i_{k-1} m)} : 1^{(i_k m)}$ as multicombining networks (MCNs). In addition, we define the simplest MCNs with $m = 1$ as FCNs. By means of Eq. (5), one can obtain the dispersion relation of the MCN as follows:

$$\begin{aligned} f_m(k) &= 2 \cdot \frac{mi_k \cot(kd_1) + \sum_{j=1}^{k-1} mi_j \cot(n_j k d_1)}{mi_k \csc(kd_1) + \sum_{j=1}^{k-1} mi_j \csc(n_j k d_1)} \\ &= 2 \cdot \frac{i_k \cot(kd_1) + \sum_{j=1}^{k-1} i_j \cot(n_j k d_1)}{i_k \csc(kd_1) + \sum_{j=1}^{k-1} i_j \csc(n_j k d_1)}. \end{aligned} \tag{10}$$

Similarly, the dispersion relation of the fundamental combining network is

$$\begin{aligned} f_1(k) &= 2 \cdot \frac{i_k \cot(kd_1) + \sum_{j=1}^{k-1} i_j \cot(n_j k d_1)}{i_k \csc(kd_1) + \sum_{j=1}^{k-1} i_j \csc(n_j k d_1)} \\ &= f_m(k). \end{aligned} \tag{11}$$

Evidently, the dispersion relations of MCNs of this kind are all the same and are the same as that of the fundamental combining network. Therefore, the properties of their photonic bands are identical and they are completely equivalent to each other. According to this characteristic, people can simplify these networks or the systems which contain the subnetworks of this kind.

For example, we calculate the two networks with $3^{(1)}$:$2^{(2)}$:$1^{(3)}$ and $3^{(3)}$:$2^{(6)}$:$1^{(9)}$, respectively. The band structures and $f(k)$ spectra are shown in Fig. 3. Obviously, one can see that the photonic bands of the two networks in Figs. 3(a) and 3(b) are identical and the $f(k)$ spectra of the two networks in Figs. 3(c) and 3(d) are all the same. This indicates that the two networks are completely equivalent. The numerical results are accordant with the analytic results.

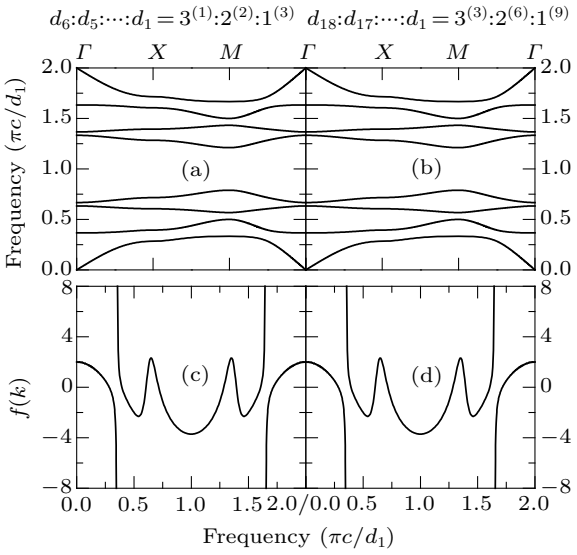


Fig. 3. Spectra of MCNs with d_6:d_5:…:$d_1 = 3^{(1)}$:$2^{(2)}$:$1^{(3)}$ and d_{18}:d_{17}:…:$d_1 = 3^{(3)}$:$2^{(6)}$:$1^{(9)}$. (a) and (b) Band structures. They are all the same. (c) and (d) $f(k)$ spectra. They are equivalent.

When $n_1 = n_2 = \cdots = n_{k-1} = n$, we call these MCNs repetitive combining networks (RCNs). For simplicity, we order $i = i_1 + i_2 + \cdots + i_{k-1}$ and $j = i_k$, then the MRWLs of RCNs can be denoted as $d_{m(i+j)} : d_{m(i+j)-1} : \cdots : d_2 : d_1 = n^{(im)} : 1^{(jm)}$.

i) When $i = j$, the RCNs are equivalent to the 2SCNs with d_2:$d_1 = n$:1. n wide passbands and $n-1$ wide stopbands are produced. The width of the band near the center of band structure is $(2/n)\pi c/d_1$ and the widths of other bands are all $(1/n)\pi c/d_1$.[36]

ii) When $i \neq j$, the RCNs are equivalent to the networks with $d_{i+j} : d_{i+j-1} : \cdots : d_1 = n^{(i)} : 1^{(j)}$.

a) When n is odd, there exist

$$m_{\rm wp} = 2n-1 \tag{12}$$

wide passbands and

$$m_{\rm ws} = 2n-2 \tag{13}$$

wide stopbands. The width of the wide passband near the centre of band structure is

$$\Delta\omega_{\rm wpc} = \frac{2}{n}\cdot\frac{\pi c}{d_1}. \tag{14}$$

In addition, there are $n-1$ wide passbands which possess the same width

$$\Delta\omega_{\rm wp} = \frac{1}{n}\cdot\frac{\pi c}{d_1}, \tag{15}$$

and their central frequencies are

$$\omega_{\rm center} = \frac{4m+1}{2n}\cdot\frac{\pi c}{d_1}, \tag{16}$$

where $m = 0,1,2,\ldots,(n-3)/2,(n+2)/2,(n+4)/2,(n+6)/2,\ldots,(2n-1)/2$. Expect for the n wide passbands above, the widths of other wide passbands satisfy the following rules. When $i<j$ $(j<i)$, the widths all increase with $i:j$ $(j:i)$ decreasing and when $i:j$ $(j:i)$ tends to zero, the widths all tend to $\Delta\omega_{\rm wp} = (1/n)\pi c/d_1$.

b) When n is even, there exist

$$m_{\rm wp} = 2n \tag{17}$$

passbands and

$$m_{\rm ws} = 2n-1 \tag{18}$$

stopbands. There are n wide passbands which possess the same width

$$\Delta\omega_{\rm wp} = \frac{1}{n}\cdot\frac{\pi c}{d_1}, \tag{19}$$

and their central frequencies are

$$\omega_{\rm center} = \frac{4m+1}{2n}\cdot\frac{\pi c}{d_1}, \tag{20}$$

where $m = 0,1,2,\ldots,(n-2)/2,(n+1)/2,(n+3)/2,(n+5)/2,\ldots,(2n-1)/2$. The variation rule for the widths of other passbands is the same as the one for the case of odd n.

As examples, we calculate the $f(k)$ spectra of the eight networks with $n = 5$ and 4, $i{:}j$ = 1:9, 1:2, 3:1, and 10:1, respectively, which are shown in Fig. 4. From Fig. 4(a), one can see that for the network with $5{:}1^{(9)}$, there exist 9 wide passbands and 8 wide stopbands. The width of the wide passband near the center of band structure is $0.40000\pi c/d_1$. And the 4 wide passbands with the central frequencies of $0.10000\pi c/d_1$, $0.50000\pi c/d_1$, $1.50000\pi c/d_1$, and $1.90000\pi c/d_1$ possess the same width $0.20000\pi c/d_1$. The three networks with $5{:}1^{(2)}$, $5^{(3)}{:}1$, and $5^{(10)}{:}1$ possess the same properties. From Fig. 4(b), it can be seen that for the network with $4{:}1^{(9)}$, 8 wide passbands and 7 wide stopbands are created. There are 4 wide passbands, which possess the identical width $0.25000\pi c/d_1$. Their central frequencies are, respectively, $0.12500\pi c/d_1$, $0.62500\pi c/d_1$, $1.37500\pi c/d_1$, and $1.87500\pi c/d_1$. The three networks with $4{:}1^{(2)}$, $4^{(3)}{:}1$, and $4^{(10)}{:}1$ possess the same characteristics. In addition, in Fig. 4(a), the widths of the four wide passbands generated from the four networks with $5{:}1^{(9)}$, $5{:}1^{(2)}$, $5^{(3)}{:}1$, and $5^{(10)}{:}1$, respectively, in the frequency range of $(0.20000-0.40000)\pi c/d_1$ are $0.15455\pi c/d_1$, $0.06174\pi c/d_1$, $0.09357\pi c/d_1$, and $0.15848\pi c/d_1$, respectively. It suggests that when $i<j$ $(j<i)$, the widths of these wide passbands increase with $i:j$ $(j:i)$ decreasing and when $i:j$ $(j:i)$ tends to zero, they will all tend to $0.20000\pi c/d_1$. Similarly, there exist the same variation rules for the widths of the four wide passbands produced in the frequency range of $(1.50000-1.75000)\pi c/d_1$ in Fig. 4(b), and when $i:j$ $(j:i)$ tends to zero, the widths will all tend to $0.25000\pi c/d_1$. Numerical results are accordant with the aforementioned formulae.

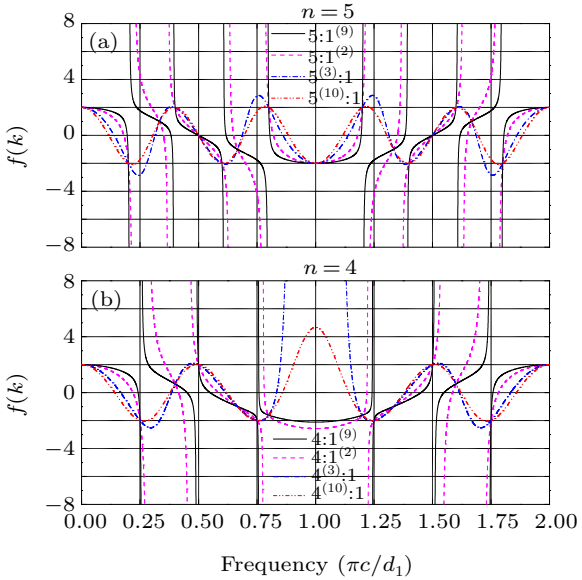


Fig. 4. (color online) $f(k)$ spectra of RCNs. In both spectra the black solid, magenta dashed, blue dash-dot, and red dash-dot-dot lines are the results of $(i,j) = (1,9)$, $(1,2)$, $(3,1)$, and $(10,1)$, respectively. (a) $n = 5$. (b) $n = 4$.

3.2. Networks with non-integer MRWLs

For actual waveguide networks, influenced by environmental temperature, pressure, material shape difference, and other factors, the integer attribute of MRWL would be easily broken, and then a mutation will occur in the phase difference and the resonances (antiresonances) created by destructive (instructive) interference will mutate into strong antiresonances (resonances).[36] Consequently, narrow passbands (stopbands) are created. The properties of narrow bands generated from the MCNs with one or more breakdown in MRWLs are complicated, and it is difficult to obtain the general rules. Therefore, in this subsection we only study the properties of narrow bands for 3SCNs and RCNs with one or more breakdowns in MRWLs.

3.2.1. 3SCNs with one breakdown in MRWLs

For the networks with

$$d_3 : d_2 : d_1 = (n_1 \pm \Delta d) : n_2 : 1, \tag{21}$$

where $\Delta d \ll 1$, we have given out the results of the properties of the narrow passbands near the center and top of band structures for the three cases that $n_1 = n_2 = 1$, n_1 and n_2 are the same even number, and n_1 is an odd number greater than 1 and $n_2 = 1$.[36] As a supplement, in this paper we obtain more study results.

When $n_1 = n_2 = n$, the numbers of the narrow passbands and narrow stopbands created except the center and top of band structure are as follows:

$$m_{\rm np} = m_{\rm ns} = 2n - 2. \tag{22}$$

When we choose '$-$' from the '$\pm$' in Eq. (21), the narrow passbands and narrow stopbands are both near the upper edge of the frequencies

$$\omega = \frac{m}{n} \cdot \frac{\pi c}{d_1}, \tag{23}$$

where $m = 1, 2, \ldots, n-1, n+1, n+2, \ldots, 2n-1$. When we choose '$+$' from the '$\pm$' in Eq. (21), they are both near the lower edge of the frequencies of Eq. (23). The total widths of the adjacent narrow passbands and narrow stopbands are

$$\Delta\omega_{\rm np} + \Delta\omega_{\rm ns} = \frac{m\Delta d}{n(n \pm \Delta d)} \cdot \frac{\pi c}{d_1}, \tag{24}$$

where $m = 1, 2, \ldots, n-1, n+1, n+2, \ldots, 2n-1$. The widths of single narrow bands are approximately

$$\Delta\omega_{\rm np} \approx \frac{m\Delta d}{2n(n \pm \Delta d)} \cdot \frac{\pi c}{d_1} \approx \Delta\omega_{\rm ns}, \tag{25}$$

where $m = 1, 2, \ldots, n-1, n+1, n+2, \ldots, 2n-1$. When n is odd, a narrow passband and two narrow stopbands are created near the center of band structure $\omega = \pi c/d_1$, the total width of which is

$$\Delta\omega_{\rm np} + \Delta\omega_{\rm ns1} + \Delta\omega_{\rm ns2} = \frac{\Delta d}{n \pm \Delta d} \cdot \frac{\pi c}{d_1}. \tag{26}$$

When '$+$' is chosen in Eq. (21), a narrow passband and two narrow stopbands are produced near the top of band structure $\omega = 2\pi c/d_1$, the total width of which is

$$\Delta\omega_{\rm np} + \Delta\omega_{\rm ns1} + \Delta\omega_{\rm ns2} = \frac{2\Delta d}{n \pm \Delta d} \cdot \frac{\pi c}{d_1}. \tag{27}$$

As examples, we calculate the band structures of the four networks with $n_1 = n_2 = 2$, $\Delta d = 0.03$, and $n_1 = n_2 = 3$, $\Delta d = 0.08$, respectively, as shown in Fig. 5. From Fig. 5(a), one can see that for the network with 1.97:2:1, there are 2 narrow passbands and 2 narrow stopbands except the center and top of band structure, whose frequencies are $(0.50375 - 0.50761)\pi c/d_1$, $(1.50000 - 1.51153)\pi c/d_1$, $(0.50000 - 0.50375)\pi c/d_1$, and $(1.51153 - 1.52284)\pi c/d_1$, respectively. The total widths of the adjacent narrow passbands and narrow stopbands are, respectively, $0.00761\pi c/d_1$ and $0.02284\pi c/d_1$. The widths of the narrow passbands are $0.00386\pi c/d_1$ and $0.01153\pi c/d_1$, respectively, while those of the narrow stopbands are, respectively, $0.00375\pi c/d_1$ and $0.01131\pi c/d_1$. Similarly, in Fig. 5(b), for the network with 2.03:2:1, there also exist 2 narrow passbands and 2 narrow stopbands except the center and top of band structure, whose frequencies are, respectively, $(0.49626 - 0.50000)\pi c/d_1$, $(1.47783 - 1.48903)\pi c/d_1$, $(0.49261 - 0.49626)\pi c/d_1$, and $(1.48903 - 1.50000)\pi c/d_1$. The total widths of adjacent narrow passbands and narrow stopbands are $0.00739\pi c/d_1$ and $0.02217\pi c/d_1$, respectively. The widths of the narrow passbands are, respectively, $0.00374\pi c/d_1$ and $0.01120\pi c/d_1$, while those of the narrow stopbands are $0.00365\pi c/d_1$ and $0.01097\pi c/d_1$, respectively. Furthermore, from Figs. 5(c) and 5(d), it is found that in the network with 2.92:3:1 (3.08:3:1), a narrow passband and two narrow stopbands are created near the center of band structure, and the total width of them is $0.02740\pi c/d_1$ ($0.02597\pi c/d_1$). In addition, from Figs. 5(b) and 5(d) it can be seen that in the network with 2.03:2:1 (3.08:3:1), a narrow passband and two narrow stopbands are produced near the top of band structure with the total width of $0.02956\pi c/d_1$ ($0.05195\pi c/d_1$). Numerical results are coincident with Eqs. (22)–(27).

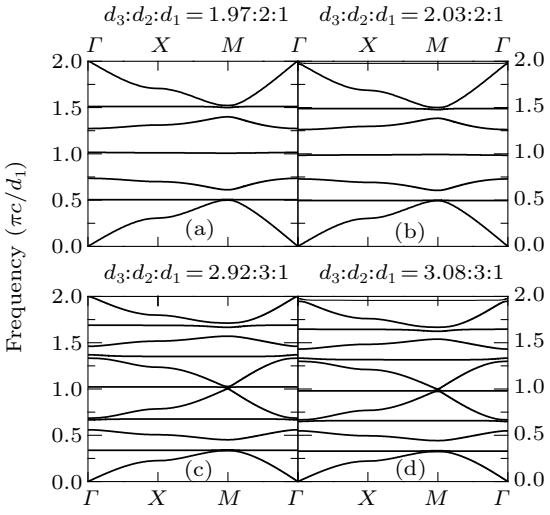


Fig. 5. Band structures of 3SCNs: (a) d_3:d_2:d_1 = 1.97:2:1, (b) d_3:d_2:d_1 = 2.03:2:1, (c) d_3:d_2:d_1 = 2.92:3:1, and (d) d_3:d_2:d_1 = 3.08:3:1.

When n_1 is even and $n_2 = 1$, a narrow passband can be created near the center of band structure, and its width is

$$\Delta\omega_{\rm np} = \frac{\Delta d}{n \pm \Delta d} \cdot \frac{\pi c}{d_1}. \tag{28}$$

As examples, Fig. 6 shows the band structures of the two networks both with $n_1 = 2$, $n_2 = 1$, and $\Delta d = 0.04$. From the figure, it can be seen that in the network with 1.96:1:1 (2.04:1:1), a narrow passband with the width of $0.02041\pi c/d_1$ ($0.01961\pi c/d_1$) is produced near the center of band structure. Numerical results accord with Eq. (28).

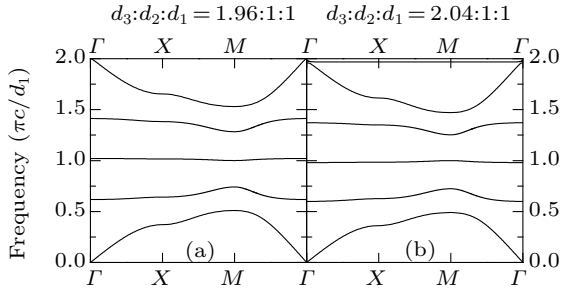


Fig. 6. Band structures of 3SCNs: (a) d_3:d_2:d_1 = 1.96:1:1, and (b) d_3:d_2:d_1 = 2.04:1:1.

3.2.2. RCNs with one breakdown in MRWLs

For the networks with

$$d_{i+j} : d_{i+j-1} : \cdots : d_2 : d_1 = (n \pm \Delta d) : n^{(i-1)} : 1^{(j)}, \quad (29)$$

where $i + j > 3$ and $\Delta d \ll 1$, we obtain the following properties of photonic bands.

When $i \neq 1$ and $i \neq j$, the networks determined by Eq. (29) and those dependent on Eq. (21) with $n_1 = n_2 = n$ all possess the following characteristics. The numbers of the narrow passbands and narrow stopbands produced except the center and top of band structures are as follows:

$$m_{\rm np} = m_{\rm ns} = 2n - 2. \quad (30)$$

When we choose '$-$' from the '$\pm$' in both Eqs. (21) and (29), the narrow passbands and narrow stopbands are both near the upper edge of the frequencies

$$\omega = \frac{m}{n} \cdot \frac{\pi c}{d_1}, \quad (31)$$

where $m = 1, 2, \ldots, n-1, n+1, n+2, \ldots, 2n-1$. When we choose '$+$' from the '$\pm$' in both Eqs. (21) and (29), they are both near the lower edge of the frequencies of Eq. (31). The total widths of the adjacent narrow passbands and narrow stopbands are

$$\Delta\omega_{\rm np} + \Delta\omega_{\rm ns} = \frac{m\Delta d}{n(n \pm \Delta d)} \cdot \frac{\pi c}{d_1}, \quad (32)$$

where $m = 1, 2, \ldots, n-1, n+1, n+2, \ldots, 2n-1$. When $j = 1$ and '$-$' ('$+$') is chosen in Eq. (29), their width ratios are approximatively $1 : (i-1)$ ($(i-1) : 1$) and $(i-1) : 1$ ($1 : (i-1)$) in turn. For the networks determined by Eq. (21) with $n_1 = n_2 = n$, the width ratios of the adjacent narrow passbands and narrow stopbands are all approximatively 1 : 1. When n is odd, a narrow passband and two narrow stopbands are created near the center of band structure $\omega = \pi c/d_1$, and their total width is

$$\Delta\omega_{\rm np} + \Delta\omega_{\rm ns1} + \Delta\omega_{\rm ns2} = \frac{\Delta d}{n \pm \Delta d} \cdot \frac{\pi c}{d_1}. \quad (33)$$

When '$+$' is chosen in both Eqs. (21) and (29), a narrow passband and two narrow stopbands are produced near the top of band structure $\omega = 2\pi c/d_1$, and their total width is

$$\Delta\omega_{\rm np} + \Delta\omega_{\rm ns1} + \Delta\omega_{\rm ns2} = \frac{2\Delta d}{n \pm \Delta d} \cdot \frac{\pi c}{d_1}. \quad (34)$$

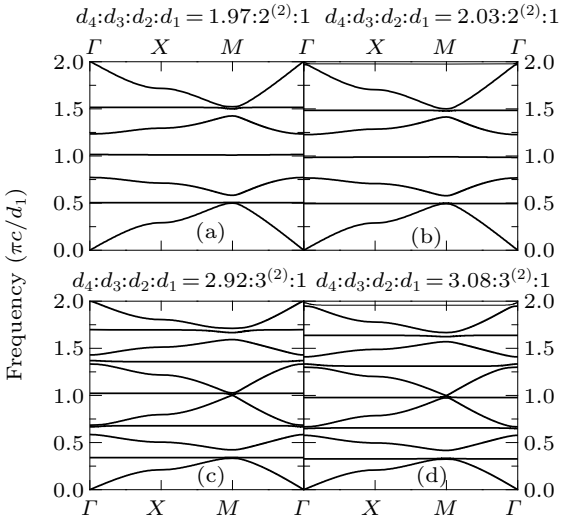


Fig. 7. Band structures of 4SCNs: (a) d_4:d_3:d_2:d_1 = 1.97:2$^{(2)}$:1, (b) d_4:d_3:d_2:d_1 = 2.03:2$^{(2)}$:1, (c) d_4:d_3:d_2:d_1 = 2.92:3$^{(2)}$:1, and (d) d_4:d_3:d_2:d_1 = 3.08:3$^{(2)}$:1.

As examples, we have calculated the four networks of $i = 3$, $j = 1$ with $n = 2$, $\Delta d = 0.03$ and $n = 3$, $\Delta d = 0.08$, respectively. The band structures are shown in Fig. 7. From Fig. 7(a), it is found that two narrow passbands and two narrow stopbands are generated by the network with $1.97 : 2^{(2)} : 1$ except the center and the top of band structure, whose frequencies are $(0.50504 - 0.50761)\pi c/d_1$, $(1.50000 - 1.51526)\pi c/d_1$, $(0.50000 - 0.50504)\pi c/d_1$, and $(1.51526 - 1.52284)\pi c/d_1$, respectively. The total widths of the adjacent narrow passbands and narrow stopbands are, respectively, $0.00761\pi c/d_1$ and $0.02284\pi c/d_1$ and their width ratios are $(0.00257\pi c/d_1) : (0.00504\pi c/d_1) \approx 1 : 2$ and $(0.01526\pi c/d_1) : (0.00758\pi c/d_1) \approx 2 : 1$, respectively. Similarly, from Fig. 7(b), it can be seen that for the network with $2.03 : 2^{(2)} : 1$, there also exist two narrow passbands and two narrow stopbands except the center and the top of the band structure, whose frequencies are, respectively, $(0.49504 - 0.50000)\pi c/d_1$, $(1.47783 - 1.48527)\pi c/d_1$, $(0.49261 - 0.49504)\pi c/d_1$, and $(1.48527 - 1.50000)\pi c/d_1$. The total widths of the adjacent narrow passbands and narrow stopbands are, respectively, $0.00739\pi c/d_1$ and $0.02217\pi c/d_1$, and their width ratios are $(0.00496\pi c/d_1) : (0.00243\pi c/d_1) \approx 2 : 1$ and $(0.00744\pi c/d_1) : (0.01473\pi c/d_1) \approx 1 : 2$, respectively. Moreover, figures 7(c) and 7(d) show that in the network with $2.92 : 3^{(2)} : 1$ ($3.08 : 3^{(2)} : 1$), a narrow passband and two narrow stopbands are created near the center of the band structure, and their total width is $0.02740\pi c/d_1$ ($0.02597\pi c/d_1$). In addition, figures 7(b) and 7(d) suggest that in the network with $2.03 : 2^{(2)}$:1 (3.08:$3^{(2)}$:1), a narrow passband and two narrow stopbands are produced near the top of the band structure with

the total width of $0.02956\pi c/d_1$ ($0.05195\pi c/d_1$). Numerical results and the formulae are consistent with each other.

When $i \neq 1$ and $i = j$, a number of narrower passbands are created, which are different from those produced by type (1) networks. When n is even, the number of the narrower passbands is

$$m_{\rm np} = n, \tag{35}$$

and they are near the frequencies

$$\omega = \frac{2m}{n+1} \cdot \frac{\pi c}{d_1}, \qquad (m = 1, 2, \ldots, n). \tag{36}$$

When n is odd, the number of the narrower passbands is

$$m_{\rm np} = n - 1, \tag{37}$$

and they are near the frequencies

$$\omega = \frac{2m}{n+1} \cdot \frac{\pi c}{d_1}, \tag{38}$$

where $m = 1, 2, 3, \ldots, (n-1)/2, (n+3)/2, (n+5)/2, (n+7)/2, \ldots, n$. The width of the narrow passband near the center of the band structure is

$$\Delta\omega_{\rm np} \approx \frac{i-1}{i} \cdot \frac{\Delta d}{n \pm \Delta d} \cdot \frac{\pi c}{d_1}, \tag{39}$$

and when '+' is chosen in Eq. (29), the width of the narrow passband near the top of the band structure is

$$\Delta\omega_{\rm np} \approx \frac{2(i-1)}{i} \cdot \frac{\Delta d}{n + \Delta d} \cdot \frac{\pi c}{d_1}. \tag{40}$$

As examples, we calculated the four networks of $i = j = 2$ with $n = 2$, $\Delta d = 0.03$ and $n = 3$, $\Delta d = 0.08$, respectively, and the band structures are presented in Fig. 8. From Figs. 8(a) and 8(b), one can see that for the two networks with $1.97{:}2{:}1^{(2)}$ and $2.03{:}2{:}1^{(2)}$, two narrower passbands are both created. In the former network, their frequencies are, respectively, $(0.66999 - 0.67011)\pi c/d_1$ and $(1.33968 - 1.34016)\pi c/d_1$, while in the latter one, those are $(0.66332 - 0.66344)\pi c/d_1$ and $(1.32634 - 1.32682)\pi c/d_1$, respectively. Similarly, from Figs. 8(c) and 8(d), it can be found that for the two networks with $2.92{:}3{:}1^{(2)}$ and $3.08{:}3{:}1^{(2)}$, there both exist two narrower passbands. The frequencies of the former ones are, respectively, $(0.50489 - 0.50522)\pi c/d_1$ and $(1.51377 - 1.51667)\pi c/d_1$, while those of the latter ones are $(0.49489 - 0.49520)\pi c/d_1$ and $(1.48373 - 1.48645)\pi c/d_1$, respectively. Furthermore, in Fig. 8(c), the width of the narrow passband near the center of the band structure is $0.01378\pi c/d_1$, and in Fig. 8(d), the widths of the two narrow passbands near the center and top of the band structure are, respectively, $0.01289\pi c/d_1$ and $0.02571\pi c/d_1$. Numerical results are accordant with Eqs. (35)–(40).

When $i = 1$ and n is even, the networks dependent on Eq. (29) possess the same characteristic as those determined by Eq. (21) with $n_1 = n_2 = n$: a narrow passband can be created near the center of band structure with the width of

$$\Delta\omega_{\rm np} = \frac{\Delta d}{n \pm \Delta d} \cdot \frac{\pi c}{d_1}. \tag{41}$$

As examples, we calculated the two networks both with $n = 2$, $\Delta d = 0.04$, and $j = 3$. The band structures are shown in Fig. 9. From the figure, it is found that in the network with $1.96{:}1^{(3)}$ ($2.04{:}1^{(3)}$), a narrow passband is produced near the center of band structure, and its width is $0.02041\pi c/d_1$ ($0.01961\pi c/d_1$). The numerical results accord with Eq. (41).

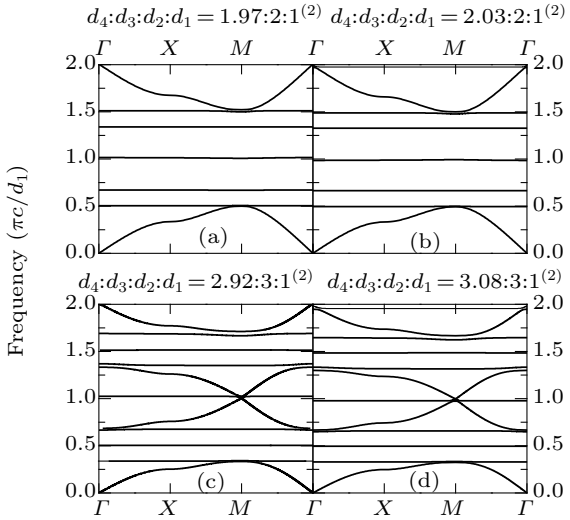


Fig. 8. Band structures of 4SCNs: (a) $d_4{:}d_3{:}d_2{:}d_1 = 1.97{:}2{:}1^{(2)}$, (b) $d_4{:}d_3{:}d_2{:}d_1 = 2.03{:}2{:}1^{(2)}$, (c) $d_4{:}d_3{:}d_2{:}d_1 = 2.92{:}3{:}1^{(2)}$, and (d) $d_4{:}d_3{:}d_2{:}d_1 = 3.08{:}3{:}1^{(2)}$.

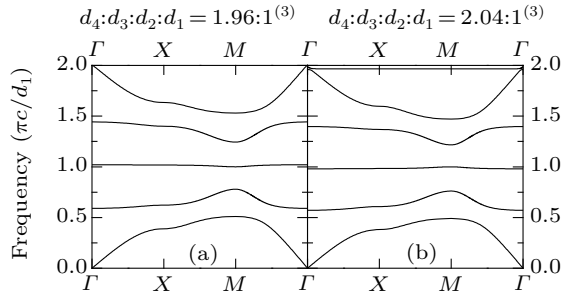


Fig. 9. Band structures of 4SCNs: (a) $d_4{:}d_3{:}d_2{:}d_1 = 1.96{:}1^{(3)}$, and (b) $d_4{:}d_3{:}d_2{:}d_1 = 2.04{:}1^{(3)}$.

3.2.3. RCNs with many breakdowns in MRWLs

For the RCNs with

$$d_{i+j} : d_{i+j-1} : \cdots : d_1 = (n \pm \Delta d)^{(i)} : 1^{(j)}, \tag{42}$$

similar to Eqs. (10) and (11), one can prove that when $i = j$ the networks determined by Eq. (42) are equivalent to 2SCNs with $(n \pm \Delta d) : 1$.

As examples, we calculated the four networks with $n = 3$, $+\Delta d = +0.09$, $i = j = 1, 3$ and $n = 4$, $-\Delta d = -0.07$, $i = j = 1, 4$, respectively. The results are shown in Fig. 10. From the

figure, it can be seen that the photonic bands of the two networks with 3.09:1 (3.93:1) and $3.09^{(3)}$:$1^{(3)}$ ($3.93^{(4)}$:$1^{(4)}$) are identical, which suggests that the two networks are equivalent. The numerical results are coincident with the analytic results.

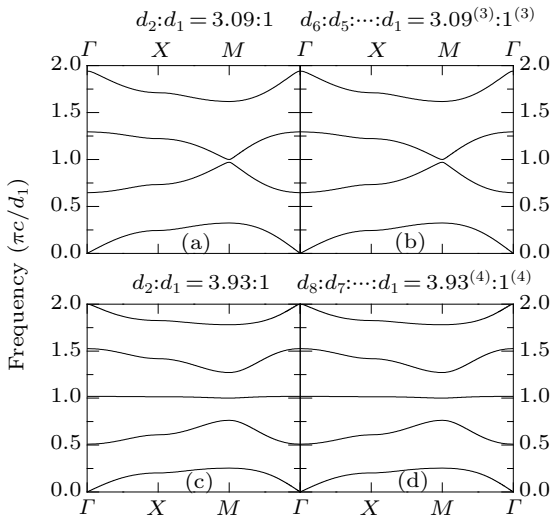


Fig. 10. The band structures of RCNs: (a) d_2:d_1 = 3.09:1, (b) d_6:d_5:⋯:d_1 = $3.09^{(3)}$:$1^{(3)}$, (c) d_2:d_1 = 3.93:1, and (d) d_8:d_7:⋯:d_1 = $3.93^{(4)}$:$1^{(4)}$.

4. Conclusions

In this work we investigated the characteristics of the photonic bands generated from the QMNs by means of the network equation and generalized dimensionless Floquet–Bloch theorem in detail.

For the networks with integer MRWLs, there only exist wide bands. For the 3SCNs with $n^i : n^j : 1$, we obtained the number formulae of the bands. For the CNs, it is found that they are equivalent to each other and they can all be simplified into the simplest FCNs. Furthermore, we obtained a series of formulae of the band number, widths, and positions for the RCNs.

When the integer attribute of MRWL is broken, there is a mutation in the phase difference and then small and strong resonances (antiresonances) occur, which result in narrow stopbands (passbands). For the networks with non-integer MRWLs, the properties of the narrow bands resulting from the breakdowns of MRWLs are studied, which cover the three cases , i.e., 3SCNs with one breakdown, RCNs with one breakdown, and RCNs with more breakdowns.

For the 3SCNs with $(n_1 \pm \Delta d) : n_2 : 1$ and $n_1 = n_2 = n$, we obtained the formulae of the number, widths, positions, and the total widths of the adjacent narrow bands except the center and top of the band structure, the formula of the total width of the central narrow bands for the case of odd n, and the formula of the total width of the top narrow bands for the case of '+' MRWLs, respectively. When n_1 is even and $n_2 = 1$, a narrow passband with the width of $[\Delta d/(n \pm \Delta d)]\pi c/d_1$ is created near the center of the bandstructure.

For the RCNs with $(n \pm \Delta d) : n^{(i-1)} : 1^{(j)}$ $(i + j > 3)$, when $i \neq 1$ and $i \neq j$, we also obtained the formulae of the number, positions, total widths, and width ratios of the adjacent narrow bands except the center and top of the band structure, the formula of the total width of the central narrow bands for the case of odd n, and the formula of the total width of the top narrow bands for the case of '+' MRWLs, respectively, which are the generalities between them and the 3SCNs with $(n \pm \Delta d) : n : 1$. When $i \neq 1$ and $i = j$, a few narrower passbands are created and the formulae of the band number and widths are obtained. Furthermore, we obtained the width formulae of the narrow passbands near the center and top of the band structure, respectively, for the case of odd n. When $i = 1$ and n is even, a narrow passband with the width of $[\Delta d/(n \pm \Delta d)]\pi c/d_1$ is created near the center of the band structures, which is the same as the characteristic of the 3SCNs with $(n \pm \Delta d) : n : 1$.

For the RCNs with $(n \pm \Delta d)^{(i)} : 1^{(j)}$, which have the properties similar to those of the RCNs with integer MRWLs, they are equivalent to the 2SCNs with $(n \pm \Delta d) : 1$.

In conclusion, according to the quantitative rules above, one can greatly simplify the CNs or the systems which contain subnetworks of this kind. The number, widths, and positions of photonic bands can be dominated more effectively by adjusting the NCWS and MRWL, and then the optical properties of the networks can be regulated. It would possess potential applications in designing all-optical devices and photonic network devices.

References

[1] John S 1987 *Phys. Rev. Lett.* **58** 2486
[2] Yablonovitch E 1987 *Phys. Rev. Lett.* **58** 2059
[3] Lin S Y, Chow E, Hietala V, Villeneuve P R and Joannopoulos J D 1998 *Science* **282** 274
[4] Noda S, Tomoda K, Yamamoto N and Chutinan A 2000 *Science* **289** 604
[5] Qi M, Lidorikis E, Rakich P T, Johnson S G, Joannopoulos J D, Ippen E P and Smith H I 2004 *Nature* **429** 538
[6] Vlasov Y A, O'Boyle M, Hamann H F and McNab S J 2005 *Nature* **438** 65
[7] Xu X S, Wang Y Q, Han S Z, Cheng B Y and Zhang D Z 2004 *Chin. Phys.* **13** 1474
[8] Che M, Zhou Y S, Wang F H and Gu B Y 2005 *Acta Phys. Sin.* **54** 4770 (in Chinese)
[9] Xie Y T and Yang L X 2011 *Chin. Phys. B* **20** 060201
[10] Wang C, Zhou C Z and Li Z Y 2011 *J. Opt.* **13** 055101
[11] Zhou M, Chen X S, Xu J, Zeng Y, Wu Y R, Lu W, Wang L W and Chen Y 2005 *Acta Phys. Sin.* **54** 411 (in Chinese)
[12] Al-Wahsh H, Boudouti E H E, Djafari-Rouhani B, Akjouj A and Dobrzynski L 2007 *Phys. Rev. B* **75** 125313
[13] Rauh H, Yampolskaya G I and Yampolskii S V 2012 *J. Opt.* **14** 015101
[14] McGurn A R 2000 *Phys. Rev. B* **61** 13235
[15] Chan T Y M and John S 2008 *Phys. Rev. A* **78** 033812

[16] Zhou C Z, Liu Y Z and Li Z Y 2010 *Chin. Phys. Lett.* **27** 084203
[17] Dong J W, Hu X H and Wang H Z 2007 *Chin. Phys.* **16** 1057
[18] Kocaman S, Chatterjee R, Panoiu N C, McMillan J F, Yu M B, Osgood R M, Kwong D L and Wong C W 2009 *Phys. Rev. Lett.* **102** 203905
[19] Kang X L, Li G J and Li Y P 2009 *J. Opt. Soc. Am. B* **26** 60
[20] Noda S, Chutinan A and Imada M 2000 *Nature* **407** 608
[21] Huang X Q and Cui Y P 2003 *Chin. Phys. Lett.* **20** 1721
[22] Zhou K Y, Guo Z Y, Muhammad A A and Liu S T 2010 *Chin. Phys. B* **19** 014201
[23] Shchesnovich V S 2007 *Phys. Rev. B* **76** 115130
[24] Guo X and Ren Z 2011 *Phys. Rev. A* **83** 013809
[25] Zhang Z Q, Wong C C, Fung K K, Ho Y L, Chan W L, Kan S C, Chan T L and Cheung N 1998 *Phys. Rev. Lett.* **81** 5540
[26] Dobrzynski L, Akjouj A, Djafari-Rouhani B, Vasseur J O and Zemmouri J 1998 *Phys. Rev. B* **57** 9388
[27] Cheung S K, Chan T L, Zhang Z Q and Chan C T 2004 *Phys. Rev. B* **70** 125104
[28] Wang Z Y and Yang X 2007 *Phys. Rev. B* **76** 235104
[29] Xiao Q, Yang X, Lu J and Liu C 2012 *Opt. Commun.* **285** 3775
[30] Li M, Liu Y and Zhang Z Q 2000 *Phys. Rev. B* **61** 16193
[31] Mir A, Akjouj A, Vasseur J O, Djafari-Roubani B, Fettouhi N, Boudouti E H El, Dobrzynski L and Zemmouri J 2003 *J. Phys.: Condens. Matter* **15** 1593
[32] Stoytchev M and Genack A Z 1997 *Phys. Rev. B* **55** R8617
[33] Bianucci P, Fietz C R, Robertson J W, Shvets G and Shih C K 2008 *Phys. Rev. A* **77** 053816
[34] Lu J, Yang X, Zhang G and Cai L 2011 *Phys. Lett. A* **375** 3904
[35] Aközbek N and John S 1998 *Phys. Rev. E* **58** 3876
[36] Song H H and Yang X B 2010 *Chin. Phys. B* **19** 074213
[37] Zhang Z Q and Sheng P 1994 *Phys. Rev. B* **49** 83